Supporting Information

Revisiting the Roles of Dopant on g-C_3N_4 Nanostructures for Piezo-photocatalytic Production of H_2O_2: A Case Study of Selenium and Sulfur

Dat Do Tran[1,2,3,+], Hoai-Thanh Vuong[1,2,3,4,+], Duc-Viet Nguyen[1,2,3,5], Pho Phuong Ly[1,2,3], Pham Duc Minh Phan[1,2,3], Vu Hoang Khoi[1.2.3.5], Phong Thanh Mai[1,2,3], and Nguyen Huu Hieu[1,2,3,*]

[1]VNU-HCM, Key Laboratory of Chemical Engineering and Petroleum Processing (Key CEPP Lab), Ho Chi Minh City University of Technology (HCMUT), 268 Ly Thuong Kiet Street, District 10, Ho Chi Minh City, Vietnam

[2]Faculty of Chemical Engineering, Ho Chi Minh City University of Technology (HCMUT)

268 Ly Thuong Kiet Street, District 10, Ho Chi Minh City, Vietnam

[3]Vietnam National University Ho Chi Minh City (VNU-HCM), Linh Trung Ward, Thu Duc City, Ho Chi Minh City, Vietnam

[4] Department of Chemistry and Biochemistry, University of California Santa Barbara (UCSB), Santa Barbara, California 93106, USA

[5]School of Chemical Engineering, University of Ulsan, Ulsan, South Korea

*Corresponding author's contact: nhhieubk@hcmut.edu.vn

Materials

Melamine ($C_3H_6N_6$), urea (CH_4N_2O), thiourea ($SC(NH_2)_2$), sulfur powder (S powder), selenium powder (Se powder), selenium dioxide (SeO_2), isopropanol (IPA), potassium iodide (KI), potassium hydrogen phthalate ($C_8H_5KO_4$), ammonium chloride (NH_4Cl), benzoquinone (BQ), and methanol (CH_3OH), were purchased from Xilong Scientific, China. Distilled water was used in the whole research. All chemicals were directly utilized without any purifications. The fabricated materials were named SCN, p-SCN, p-SeCN, and SeCN for the use of thiourea, sulfur power, selenium power, and SeO_2 as doping precursors, respectively. g-C_3N_4 was prepared by the same method without the presence of other agents and denoted as GCN.

Characterization

The optical features of all materials were computed by UV-vis diffuse reflectance spectroscopy (UV-DRS). The characteristic crystal structure of materials was characterized by X-ray diffraction (XRD). The morphologies of materials were also examined by field emission scanning electron microscopy (FESEM) and high-resolution transmission electron microscopy (HRTEM). Furthermore, the surface charge and conductivity of the materials were detected by zeta potential measurements. The BET and Barret-Joyner-Halender (BJH) methods were carried out using N_2 adsorption-desorption measurements to determine the specific surface area, pore size, and pore volume of all samples. Thermogravimetric analysis (TGA) was obtained to analyze the thermal stability of materials. Fourier transform infrared (FTIR) and solid-state nuclear magnetic resonance spectroscopy (ssNMR) were employed to characterize functional groups and molecular structure. In addition, XPS was performed to determine the chemical states with the spectra of all samples. In order to analyze the recombination of charges and the charge transfer resistance, photoluminescence (PL) spectra and electrochemical impedance spectroscopy (EIS) were utilized. XPS-VB spectra were conducted to identify the valance band (VB) edge of the materials and Mott-Schottky plots were used to confirm the

position of the flat-band potential of the materials. Cyclic voltammetry (CV) and linear sweep voltammetry (LSV) were also performed in the study to study the electrocatalytic properties of the materials.

Table S1. Summary of the photocatalytic process for the production of H_2O_2

Photocatalyst	**Light source**	**Experimental conditions**	**H_2O_2 yield**	**Ref.**
GCN	Two 50 W Philips halogen lamps	Catalyst: 1 mg Solvent: Water SA: IPA Time: 90 min Atmosphere: O_2	460.8 μM	This work
SCN			393.7 μM	
p-SCN			725.8 μM	
p-SeCN			661.1 μM	
SeCN			903.01 μM	
C, O co-doped g-C_3N_4	300 W Xenon arc lamp	Catalyst: 100 mg Solvent: Water SA: IPA Time: 30 h Atmosphere: O_2	60.3 μmol	[1]
B doped g-C_3N_4 tubes	300 W xenon lamp	Catalyst: 50 mg Solvent: Water SA: IPA	42.31 μM min^{-1}	[2]
P doped g-C_3N_4 tubes			24.95 μM min^{-1}	

S doped g-C3N4 tubes		Time: 120 min Atmosphere: O_2	24.22 μM min^{-1}	
Ultra-thin g-C_3N_4	AM 1.5 (100 mW cm^{-2}, 400 nm ≤ λ ≤ 760 nm)	Catalyst: 20 mg Solvent: Water SA: IPA Time: 5 h Atmosphere: O_2	665.4 μmol h^{-1} g^{-1}	[3]
K-, P-, O-, and S-co-doped g-C_3N_4	300 W Xenon lamp	Catalyst: 150 mg Solvent: Water SA: IPA Time: 180 min Atmosphere: O_2	6231 μM	[4]
Cl doped g-C_3N_4 nanorods	250 W high-pressure sodium lamp	Catalyst: 200 mg Solvent: Water SA: EDTA Time: 6 h Atmosphere: O_2	0.35 mmol·L^{-1}	[5]
Br doped g-C_3N_4 nanorods			1.99 mmol·L^{-1}	
Ultrathin g-C_3N_4 nanosheet	Simulated sunlight irradiation system	Catalyst: 50 mg Solvent: Water SA: Ethanol	1083 μmol $g^{-1}h^{-1}$	[6]

		Time: 180 min Atmosphere: O_2		
CN-vacancy-doped g-C_3N_4	300 W Xenon lamp	Catalyst: 50 mg Solvent: Water SA: IPA Atmosphere: O_2 Time: 60 min	718.36 $\mu mol\ g^{-1}\ h^{-1}$	[7]
KOH doped g-C_3N_4	500 W Xe arc lamp	Catalyst: 30 mg Solvent: Water SA: IPA Atmosphere: O_2 Time: 240 min	704 $\mu mol\ g^{-1}\ h^{-1}$	[8]
K and P doped g-C_3N_4	300 W Xenon lamp	Catalyst: 20 mg Solvent: Water SA: EtOH Atmosphere: O_2	216 $\mu mol\ g^{-1}\ h^{-1}$	[9]
P doped g-C_3N_4	Blue LED light	Catalyst: 50 mg Solvent: Water SA: Ethanol Atmosphere: O_2	285.34 $\mu mol\ L^{-1}$	[10]

		Time: 180 min		
B and O co-doped $g\text{-}C_3N_4$	300 W Xenon lamp	Catalyst: 40 mg Solvent: Water SA: Ethanol Atmosphere: O_2 Time: 150 min	620 $\mu mol\ g^{-1}\ h^{-1}$	[11]
O doped $g\text{-}C_3N_4$	300 W Xenon lamp	Catalyst: 50 mg Solvent: Water SA: Isopropanol Atmosphere: O_2	2008.4 $\mu mol\ g^{-1}\ h^{-1}$	[12]

Table S2. Elemental percentage as-prepared samples

Sample	C	N	O	Cl	X	(Se)
GCN	44.78[a]	53.77[a]	1.35[a]	0.1[a]	-	-
SCN	43.96[a]	53.9[a]	1.83[a]	0.12[a]	0.19[a]	-
p-SCN	44.36[a]	52.89[a]	1.91[a]	0.36[a]	0.27[a]	-
p-SeCN	44.53[a]	54.29[a]	1.06[a]	0.11[a]	0.01[a]	0.199
SeCN	44.17[a]	53.9[a]	1.69[a]	0.16[a]	0.08[a]	0.08

[a]Data was obtained from XPS results

[b]Data was obtained from ICP-MS results

Table S3. Physical properties of all samples

Samples	Zeta potential (mV)	Conductivity (mS/cm)	Surface Active Area ($m^2 g^{-1}$)	Pore Volume ($cm^3 g^{-1}$)	Average Pore Size (nm)	d-spacing (nm)		Average Crystallite Site (nm)
						(100)	(002)	
GCN	− 31.6	0.00604	51.136	0.222	3.4710	0.679	0.326	3.939
SCN	− 28.2	0.00824	57.224	0.277	3.5628	0.684	0.323	9.198
p-SCN	− 34.4	0.0057	54.822	0.243	3.5199	0.684	0.322	10.490
p-SeCN	− 34.3	0.0449	52.142	0.268	3.4657	0.690	0.323	9.642
SeCN	− 31.2	0.00810	58.076	0.304	4.0406	0.690	0.323	9.664

Table S4. Calculations of the delocalized π-π* electron systems based on XPS data

Sample	$(\pi\text{-}\pi^*)/C_{total}$	$(\pi\text{-}\pi^*)/N_{total}$	$N\text{-}(C_3)/C{=}N\text{-}C$
GCN	0.046	0.083	0.199
SCN	0.046	0.212	0.199
p-SCN	0.078	0.084	0.346
p-SeCN	0.059	0.059	0.341
SeCN	0.058	0.079	0.265

Table S5. Electronic properties of as-synthesized materials

Samples	Bandgap Energy (eV)	Valance Band Edge Energy (eV)	Valance Band Potential (eV)	Flat Band Potential (eV)	Work function (eV)	Conduction Band Potential (eV)	
GCN	2.68	2.03[a]	1.47[a]	-1.327[b]	5.630	-1.21[a]	-1.230[b]
SCN	2.67	2.05[a]	1.49[a]	-1.314[b]	5.617	-1.18[a]	-1.217[b]
p-SCN	2.62	1.95[a]	1.39[a]	-1.319[b]	5.622	-1.23[a]	-1.222[b]
p-SeCN	2.71	2.08[a]	1.52[a]	-1.302[b]	5.605	-1.19[a]	-1.205[b]
SeCN	2.61	2.06[a]	1.50[a]	-1.239[b]	5.542	-1.11[a]	-1.142[b]

[a] Data and values were exported and computed from XPS-VB results

[b] Data and values were exported and computed from Mott Schottky plots

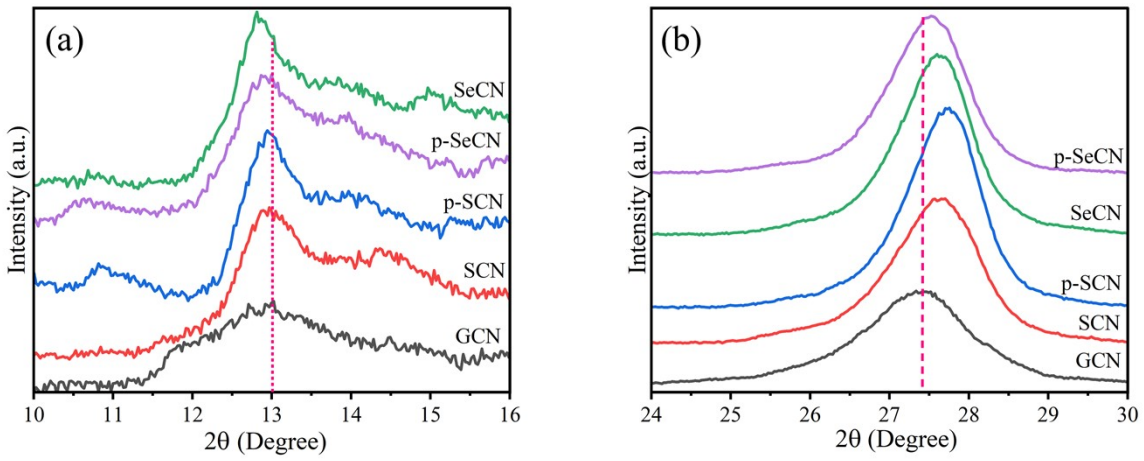

Fig. S1. XRD patterns of as-prepared materials from 10 to 16 degree (a), and from 24 to 30 degree (b)

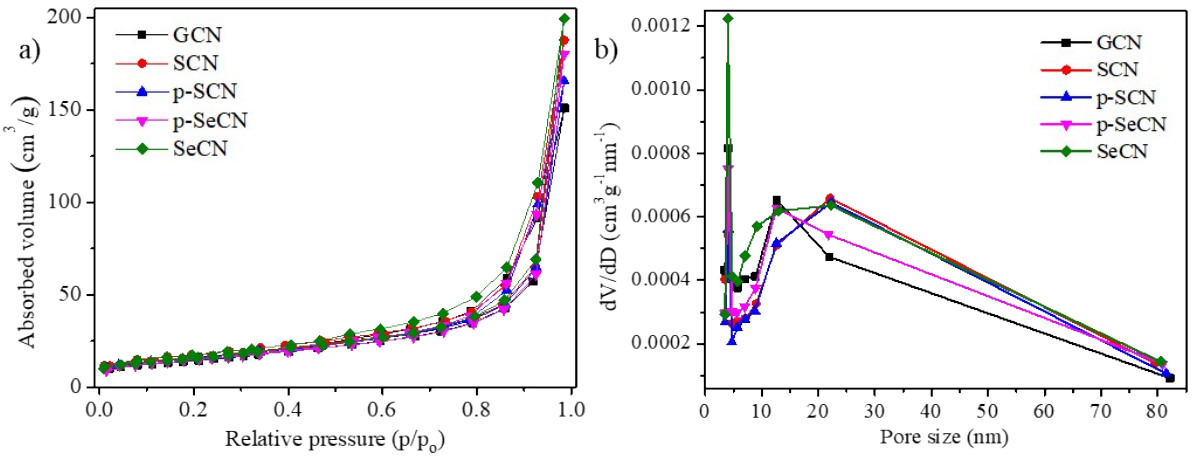

Fig. S2. N_2 adsorption-desorption isotherms of samples and (b) the pore size distribution curves of GCN, SCN, p-SCN, p-SeCN, and SeCN

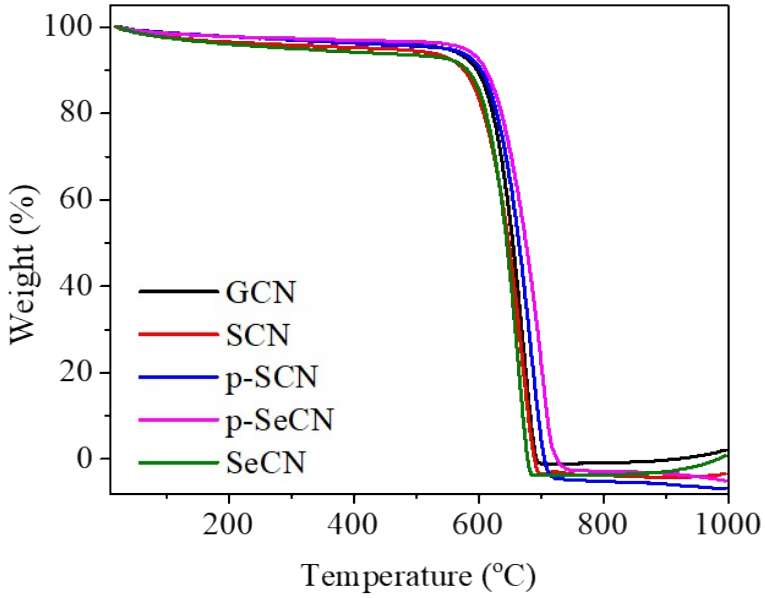

Fig. S3. TGA curves for GCN, SCN, p-SCN, p-SeCN, and SeCN

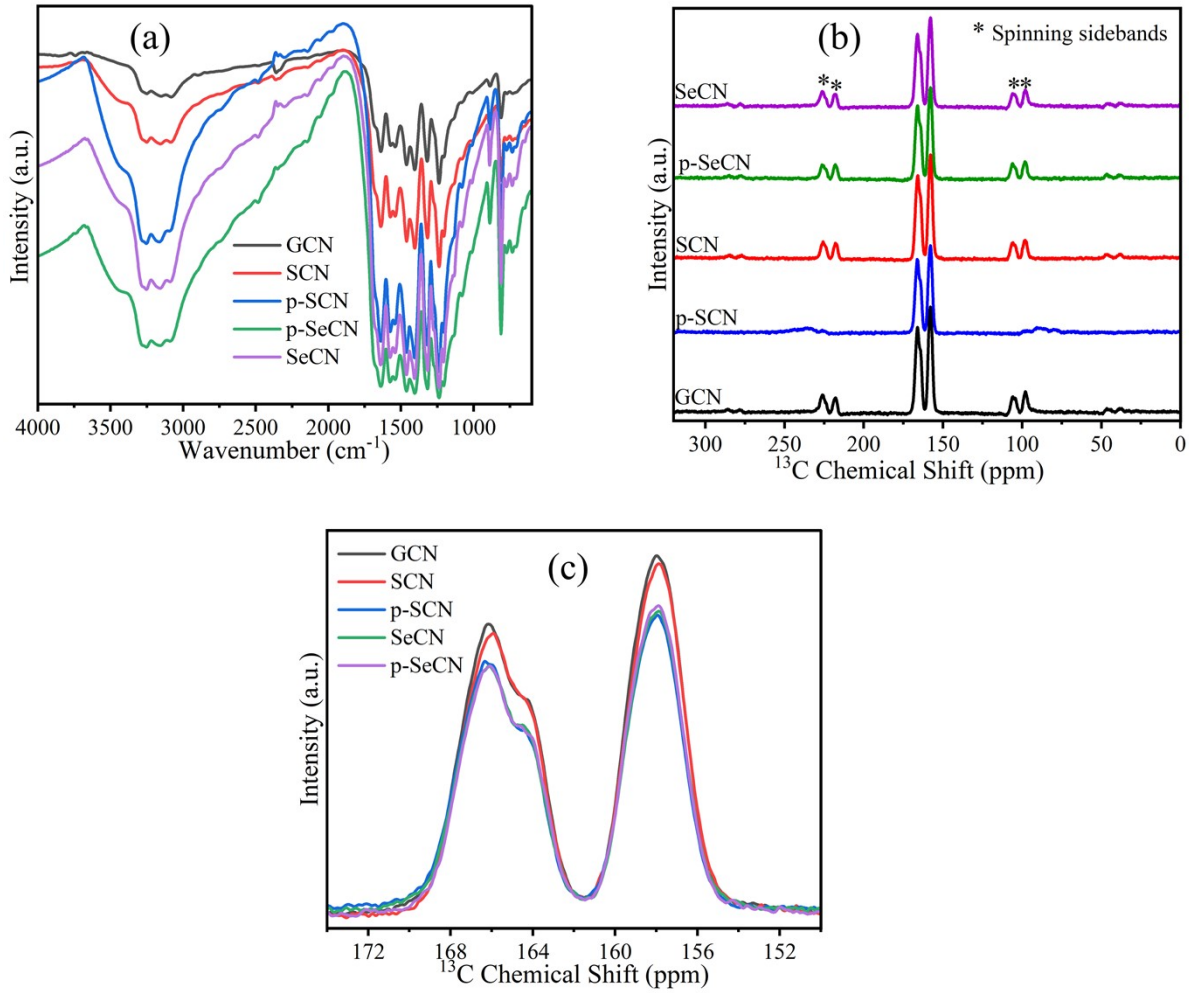

Fig. S4. FTIR (a) and ^{13}C solid-state NMR (b) and (c) spectra of the materials

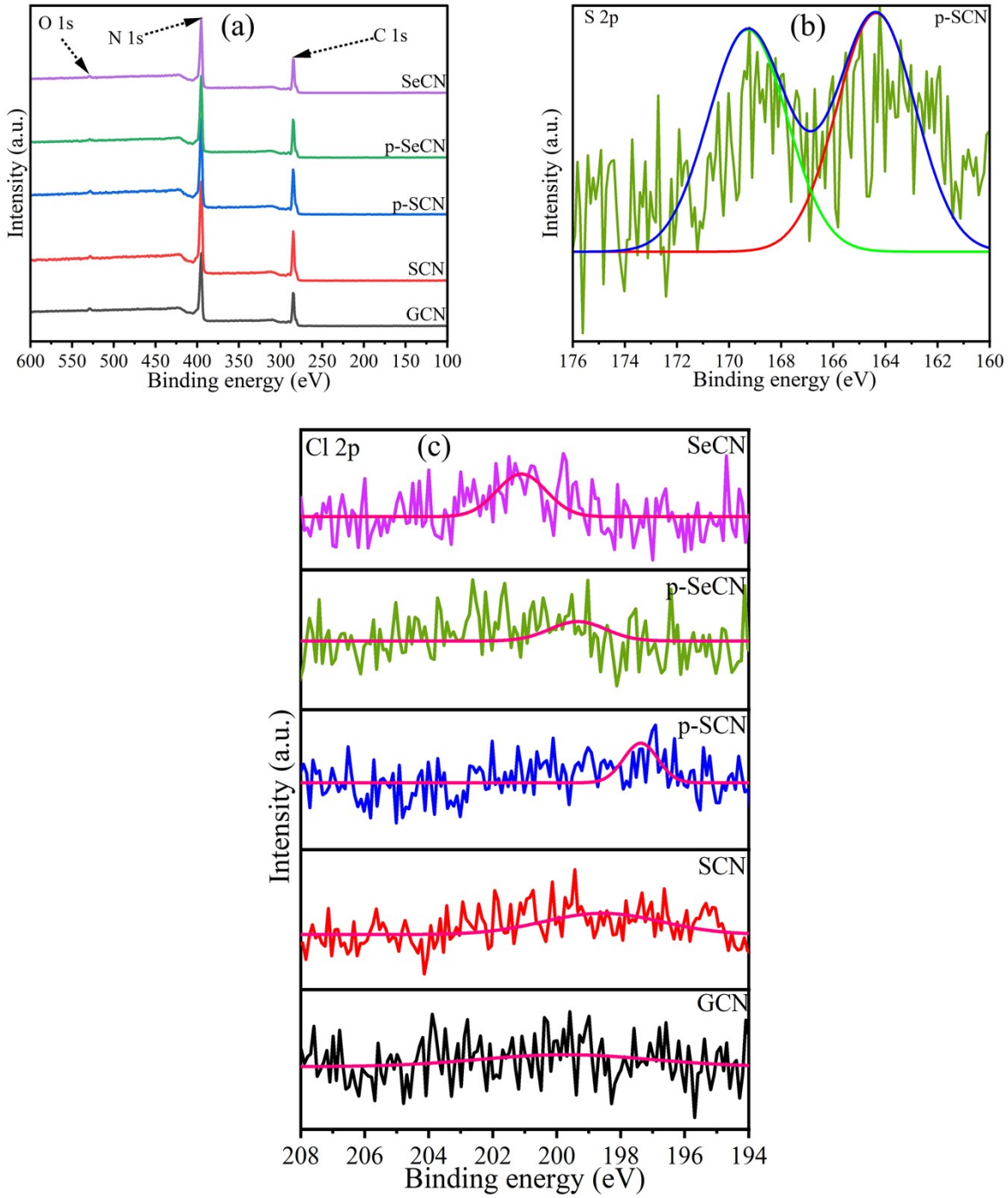

Fig. S5. XPS survey spectra of materials

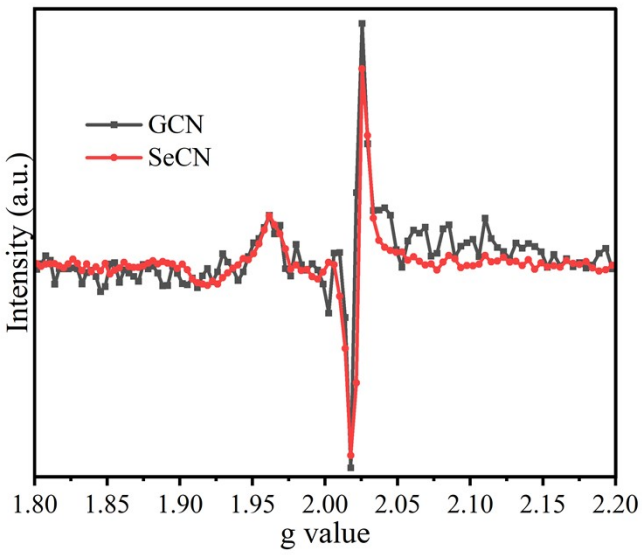

Fig. S6. EPR spectra of GCN and SeCN

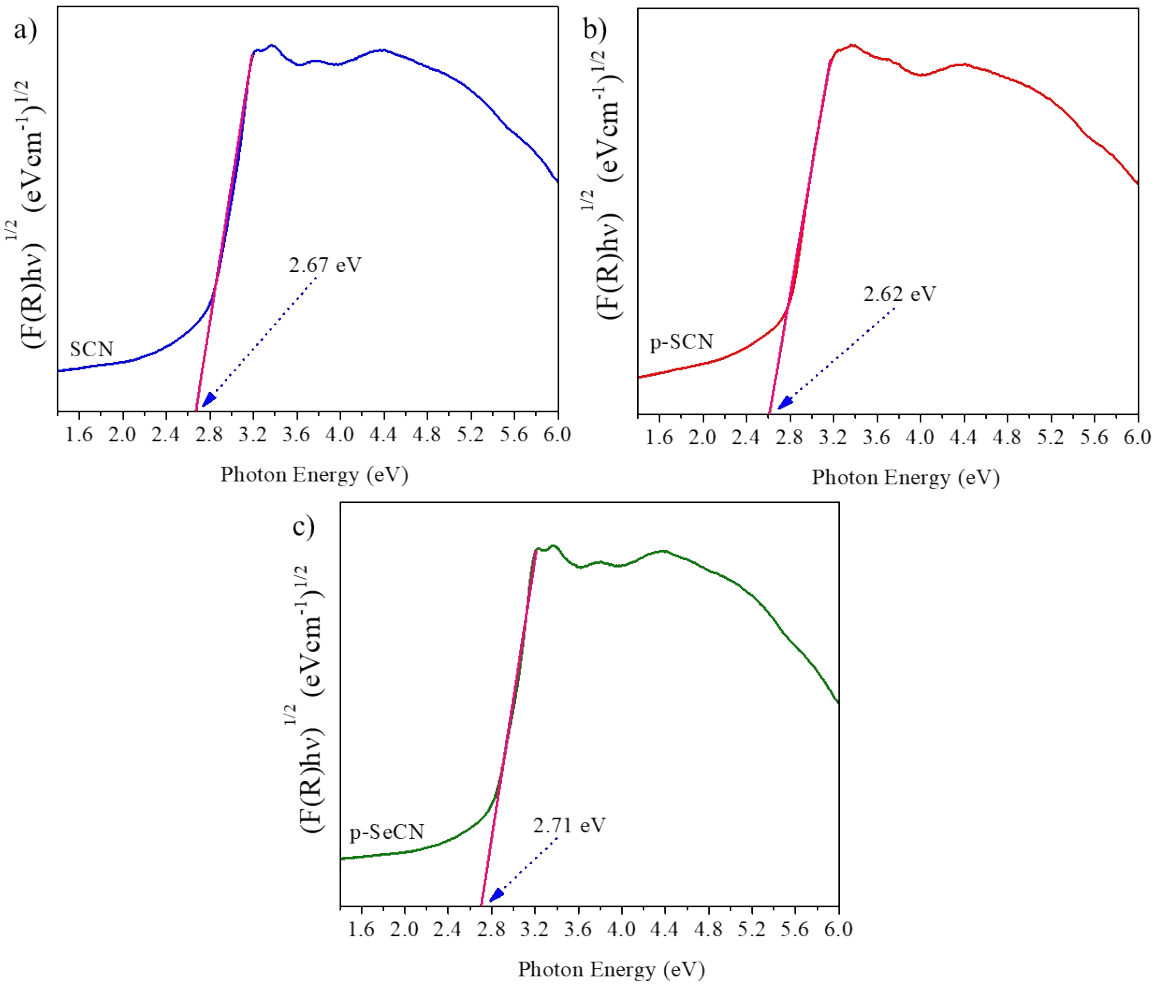

Fig. S7. Bandgap energy of SCN (a), p-SCN (b), and p-SeCN (c)

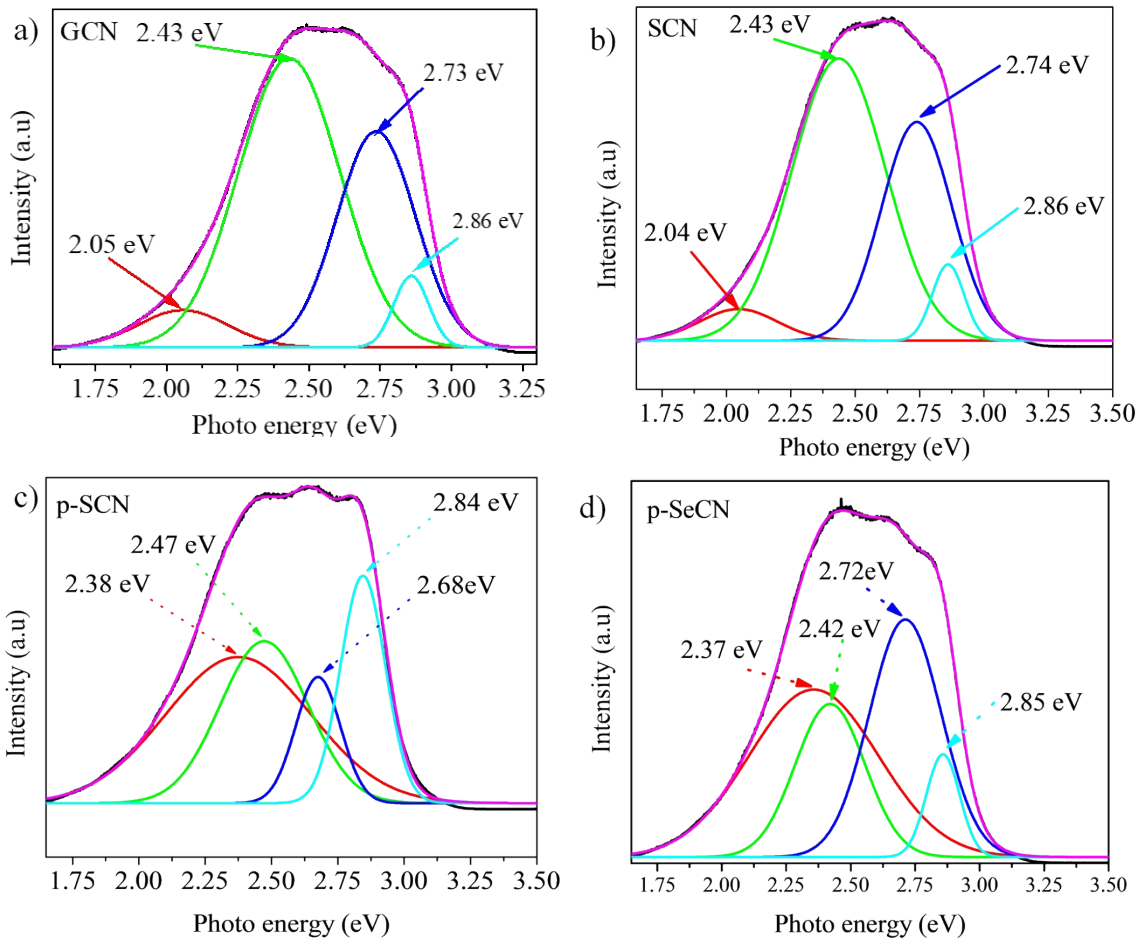

Fig. S8. PL energy of GCN (a), SCN (b), p-SCN (c), and p-SeCN (d)

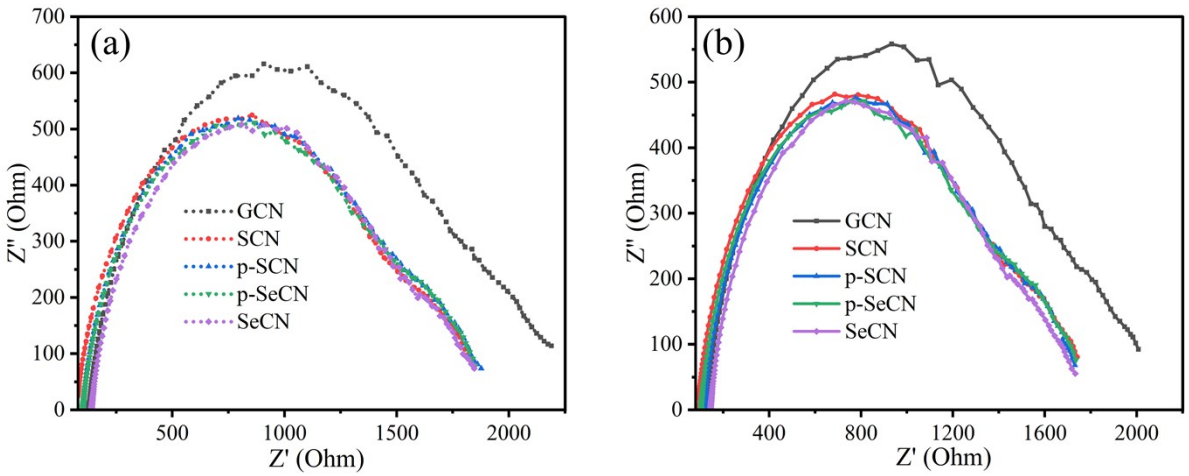

Fig. S9. EIS of GCN, SCN, p-SCN, p-SeCN, and SeCN

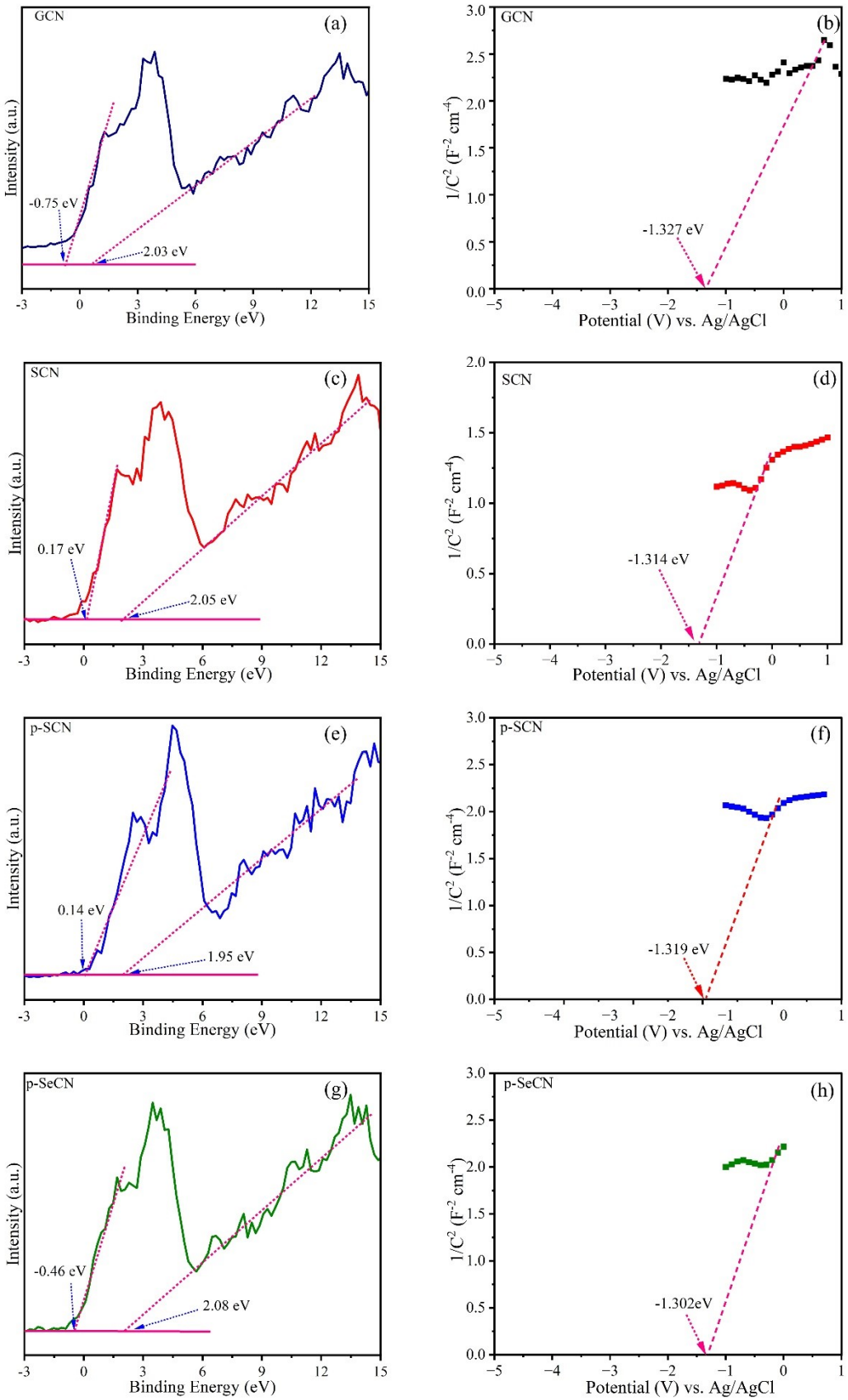

Fig. S10. XPS-VB and Mott Schottky plots of (a-b) GCN, (c-d) SCN, (e-f) p-SCN, and (g-h) p-SeCN

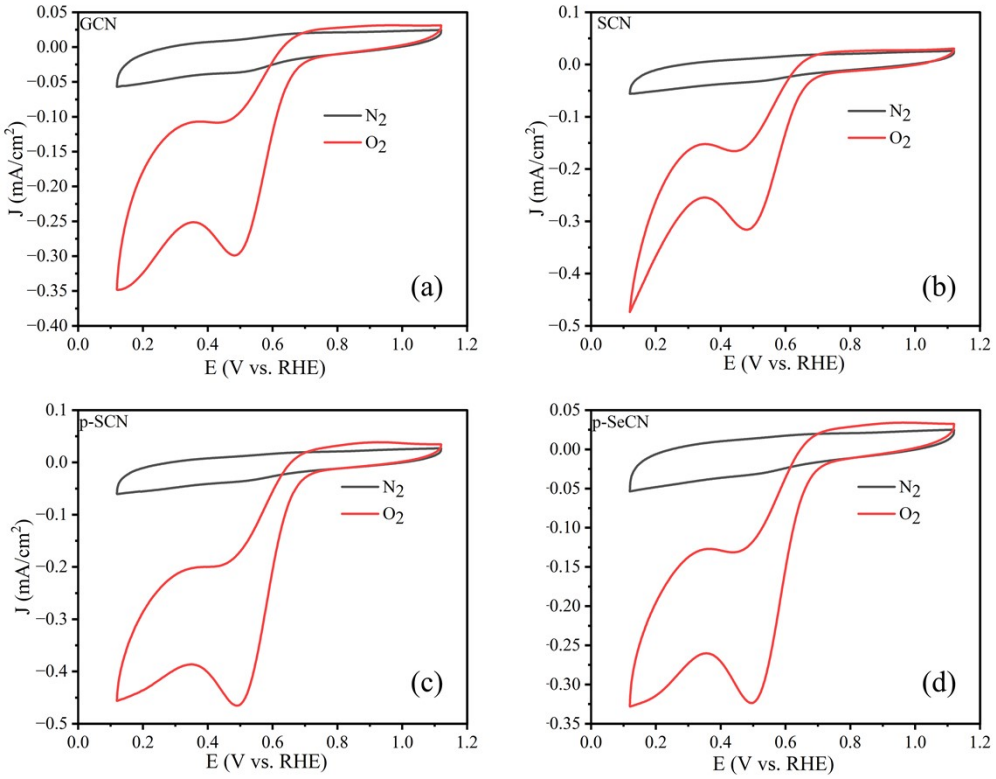

Fig. S11. CV curves of GCN (a), SCN (b), p-SCN (c), and p-SeCN (d)

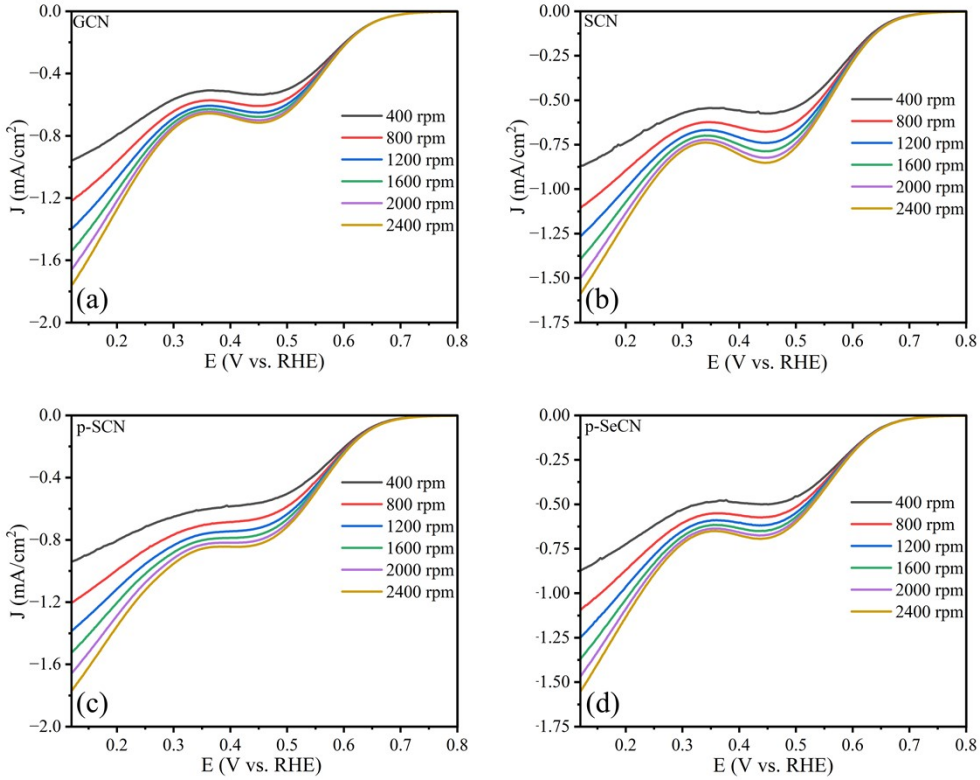

Fig. S12. LSV curves of GCN (a), SCN (b), p-SCN (c), and p-SeCN (d)

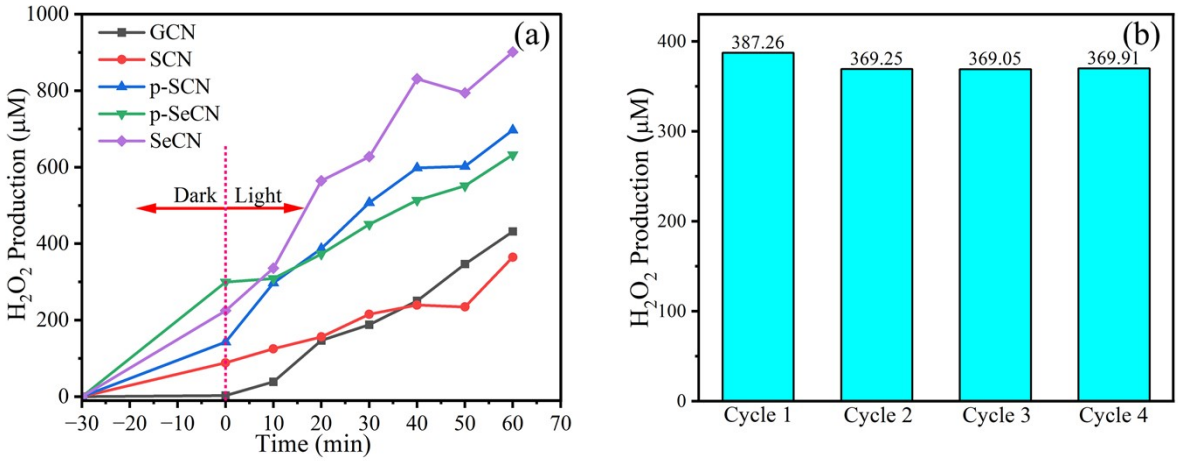

Fig. S13. (a) Piezo-photocatalytic H_2O_2 production of as-prepared samples and (b) the cycle test of 50 mg of SeCN under 1 h irradiation

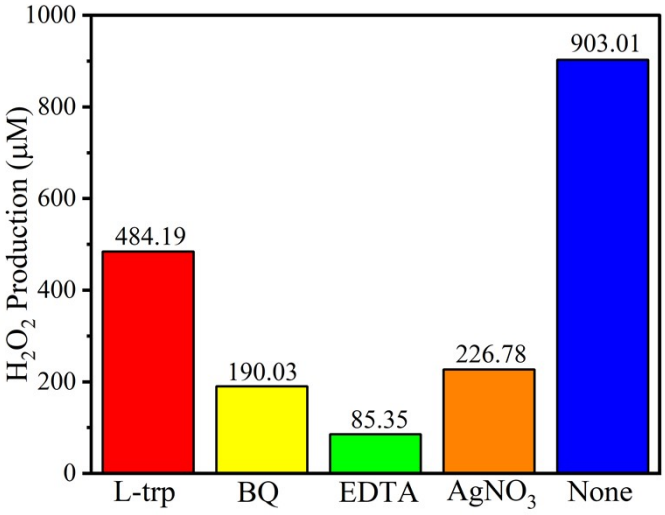

Fig. S14. Piezo-photocatalytic results of SeCN with the presence of a scavenger

References

[1] Samanta, S.; Yadav, R.; Kumar, A.; Sinha, A. K.; and Srivastava, R*Appl. Catal. B*, 2019, **259**, 118054.

[2] Liu, Y.; Zheng, Y.; Zhang, W.; Peng, Z.; Xie, H.; Wang, Y.; Huang, Y. *J. Mater. Sci. Technol.*, 2021, **95**, 127-135.

[3] Hu, J.; Zhang, P.; Yang, T.; Cai, Y.; Qu, J.; Yang, X. *Appl. Surf. Sci.*, 2022, **576**, 151841.

[4] Deng, L.; Sun, J.; Sun, J.; Wang, X.; Shen, T.; Zhao, R.; Wang, B. *Appl. Surf. Sci.*, 2022, 153586.

[5] Zhang, C.; Bai, J.; Ma, L.; Wang, F.; Zhang, X.; Hu, S. *Diamond Relat. Mater.*, 2018, **87**, 215-222.

[6] Zhou, L.; Feng, J.; Qiu, B.; Zhou, Y.; Lei, J., Xing; Zhang, J. *Appl. Catal. B*, 2020, **267**, 118396.

[7] Zhang, Z.; Zheng, Y.; Xie, H.; Zhao, J.; Guo, X.; Zhang, W.; Huang, Y. *J. Alloys Compd.*, 2022, **904**, 164028.

[8] Zhang, H.; Jia, L.; Wu, P.; Xu, R.; He, J.; Jiang, W. *Appl. Surf. Sci.*, 2020, **527**, 146584.

[9] Fattahimoghaddam, H.; Mahvelati-Shamsabadi, T.; Jeong, C. S.; Lee, B. K. *J. Colloid Interface Sci.*, 2022, **617**, 326-340.

[10] Li, D.; Wen, C.; Huang, J.; Zhong, J.; Chen, P.; Liu, H.; Liu, G. *Appl. Catal. B*, 2022, **307**, 121099.

[11] You, Q.; Zhang, C.; Cao, M.; Wang, B.; Huang, J.; Wang, Y.; Yu, G. *Appl. Catal. B*, 2023, **321**, 121941.

[12] Xie, H.; Zheng, Y.; Guo, X.; Liu, Y.; Zhang, Z.; Zhao, J.; Huang, Y. *ACS Sustainable Chem. Eng.*, 2021, **9**, 6788-6798.